Structural Engineering and Mechanics, *Vol. 63, No. 3 (2017) 385-400*
DOI: https://doi.org/10.12989/sem.2017.63.3.385

Experimental study on partially-reinforced steel RHS compression members

Seval Pinarbasi*

Department of Civil Engineering, Kocaeli University, Umuttepe Campus, Kocaeli 41380, Turkey

(Received August 30, 2016, Revised March 7, 2017, Accepted March 9, 2017)

Abstract. This paper presents an experimental study on the behavior of axially-loaded steel RHS (rectangular hollow section) compression members that are partially reinforced along their lengths with welded steel plates. 28 slender column tests were carried out to investigate the effects of the slenderness ratio of the unreinforced member and the ratio of the reinforced length of the member to its entire length. In addition to the slender column tests, 14 stub-column tests were conducted to determine the basic mechanical properties of the test specimens under uniform compression. Test results show that both the compressive strength and stiffness of an RHS member can be increased significantly compared to its unreinforced counterpart even when only the central quarter of the member is reinforced. Based on the limited test data, it can be concluded that partial reinforcement is, in general, more effective in members with larger slenderness ratios. A simple design expression is also proposed to predict the compressive strength of RHS columns partially reinforced along their length with welded steel plates by modifying the provisions of AISC 360-10 to account for the partial reinforcement.

Keywords: buckling; nonuniform member; partial reinforcement; rectangular hollow section (RHS); stepped column; steel; strengthening

1. Introduction

Members with continuously variable (tapered) or partially constant (stepped) geometrical properties (such as, thickness, cross sectional area and/or moments of inertia) have long been used in buildings and bridges, as well as in mechanical engineering and aerospace industries. Through better distribution of strength and stiffness, the use of nonuniform members may reduce the total weight of the structure significantly, which, in some special cases, may become particularly important (Saka 1997). Due to their favorable properties, many studies have been conducted in literature on nonuniform members (e.g., Park 2004, Sing and Li 2009, Park and Park 2013, Rajasekaran and Wilson 2013, Marques *et al.* 2014, Fan *et al.* 2015, Kus 2015, Surla *et al.* 2015, Zhang *et al.* 2015, Liu *et al.* 2016, Ren *et al.* 2017, etc.).

Nonuniform structural members can also be used for strengthening existing structures. For example, braces of a steel frame, girders of a bridge or truss members can be reinforced along part of their length by welding steel plates. In fact, it usually leads to more economical designs if only the partial length, instead of the entire length, of a structural member is reinforced. As stated by Timoshenko and Gere (1961), "It is evident in the case of a compressed bar with hinged ends, for example, that the stability can be increased by removing a portion of the material from the ends and increasing the cross section over the middle portion".

Although many steel structures and bridges have already been strengthened using welded steel plates, there is little published research in the literature on the behavior of reinforced steel members (Bhowmick and Grondin 2016). Since current design specifications do not include specific guidelines for reinforced steel members, design engineers dealing with such members generally use the design criteria for unreinforced members. Provided that the reinforcement is applied through the entire length of the member, the method is presumed to be safe (Wu and Grondin 2002). However, the use of such an approach may not always be proper when the reinforcement is applied only to part of the length of the member.

To the limited knowledge of author, the experimental behavior of partially reinforced steel RHS compression members along their lengths has not been studied so far. Studies in literature on reinforced steel columns have been concentrated on reinforcing wide-flange compression members with welded steel plates along their entire length. Nagaraja Rao and Tall (1962) investigated the effect of welding cover plates to a wide-flange column under load. They tested three pin-ended columns: one unreinforced, one reinforced under load (the initial stress was approximately 27% of steel yield stress) and one reinforced under no load. The test columns were 2440 mm long, with a slenderness ratio of 48. In addition to the pin-ended column tests, they conducted stub-column tests to obtain "average stress-strain curve of the cross section of the shape", which "includes the effect of residual stress and may be helpful in the prediction of column strength by the tangent modulus method". Both the stub-column and pin-ended column tests showed that since the effect of welding was "confined to a very small region in the vicinity of the weld", welding did not reduce the buckling stress in the reinforced members. They reported that the specimen reinforced under load reached

∗Corresponding author, Ph.D.
E-mail: sevalp@gmail.com

ISSN: 1225-4568 (Print), 1598-6217 (Online)

98% of its yield strength, while the ultimate capacity of the specimen reinforced under no load was 96% of its yield strength. Brown (1988) developed an analytical method for calculating the ultimate capacity of a column reinforced under load. He verified one of the main findings of Nagaraja Rao and Tall (1962) that the specimen reinforced under load had a load capacity comparable to that reinforced under no load, but also showed that this finding is not necessarily true for columns with larger slenderness ratios. Tall (1989) was concerned with reinforcing steel columns where welding is used as the reinforcement, either alone or with cover plates. He concluded that reinforcing steel columns by cover plates welded to the flanges improves the column strength as a result of the combined effect of additional material and favorable change of residual stress distribution. Tide (1990) reviewed several proposed reinforcement methods published in literature for compression members under load and explained why he disagreed with most of these procedures. He also listed the basic factors that should be considered in the design stage when reinforcing columns under load. Recently, Bhowmick and Grondin (2016) conducted a comprehensive numerical study on columns reinforced with steel cover plates welded either parallel to web or to flanges. After validating their finite element model using a comparison with the available limited test data in the literature, Bhowmick and Grondin (2016) used this model to investigate the effect of the column slenderness, initial out-of-straightness, residual stresses, preload, steel grade and the orientation of reinforcing plates. They concluded that the most important parameter affecting the reinforced column strength is the nondimensional column slenderness, which depends on both yield strength of steel and Euler elastic buckling stress for the column. Bhowmick and Grondin (2016) also concluded that change in preload (from 40% to 60% of the load carrying capacity of the unreinforced column) or change in steel grade does not appreciably affect the predicted strength-to-yield strength ratio for the reinforced columns while the effects of initial out-of-straightness and reinforcing plate orientation can be significant for intermediate and long columns. Bhowmick and Grondin (2016) also conducted a detailed statistical analysis to determine the appropriate resistance factor to use for the limit state design of columns reinforced with welded steel plates along their entire lengths.

Elastic buckling loads for *stepped* compression members can be obtained by analyzing each segment of the member separately and then solving the characteristic equation derived for the member using continuity conditions between each segment and boundary conditions at the member ends. Timoshenko and Gere (1961) derived a transcendental equation for calculating elastic buckling load for a pin-ended partially reinforced compression member. In a recent study, Pinarbasi Cuhadaroglu *et al*. (2012) revisited this buckling problem and analyzed three-segment symmetric stepped compression members with pinned ends using variational iteration method. Pinarbasi Cuhadaroglu *et al*. (2012) also listed elastic buckling loads for various stiffness and stiffened length ratios. However, the results of these analytical studies cannot directly be used in most practical designs since structural members experience inelastic buckling in many engineering applications. Also, the axial behavior of a compression member may be influenced significantly from the presence of residual stresses, initial out-of-straightness and load eccentricity (Galambos 1998). For this reason, it is convenient to accompany analytical studies with experimental studies, the results of which can also be used in validating numerical models similar to that developed by Bhowmick and Grondin (2016).

In addition to the analytical and numerical studies, Pinarbasi Cuhadaroglu *et al*. (2012) conducted an experimental study to determine the buckling loads of twelve slender steel members with rectangular hollow section (RHS), 120×40×4 mm, nine of which were reinforced along part of their length with welded steel plates. Hollow sections have widely been used in steel structures constructed in Turkey, particularly as earthquake/wind bracings and as truss members. Even though square or circular hollow sections have used more extensively as compression members, in this preliminary stage of the research program, test specimens were selected to have rectangular hollow sections so that buckling can occur in the desired direction during the experiments. The reinforced test specimens were prepared by welding steel plates, 100×3 mm, over their larger faces. Thus, the addition of the cover plates predominantly increased the minor-axis flexural rigidity of the cross section (approximately twice), which governs the flexural buckling behavior of the member. The effect of partial reinforcement was investigated by studying three different reinforcement length ratios, 0.2, 0.33 and 0.5, corresponding, respectively, to the reinforcing plates with lengths of one-fifth, one-third and one half of the entire member length (2 m). Test results show that even when very little reinforcement was applied to the member with unreinforced (reference) slenderness ratio of KL/r=125 (where the effective length factor K is unity for a member with pinned ends, L is the unsupported length of the member, and r is the minimum radius of gyration of the steel cross section), i.e., even when only one-fifth of the entire column length was reinforced, the capacity of the member increased by approximately 30%. When the central half of the column was reinforced, the capacity increase was approximately 50%. The results of this study were promising but not sufficient to derive a preliminary design expression for similar reinforced members since only one parameter that controls the capacity of the member was investigated; the reinforcement length ratio. Since the unreinforced cross section was identical in all tested reinforced members, additional tests are required to study the effect of member slenderness ratio, which may have a great influence on the type of global buckling, elastic or inelastic. Similarly, the behavior of the members with reinforcement length ratio greater than 0.5 is to be studied to have a complete set of experimental data.

The main objective of this paper is to investigate the compressive behavior of steel RHS compression members reinforced along part of their length with welded steel plates through a comprehensive experimental study. With this aim, 6 unreinforced (reference) and 22 partially-reinforced steel

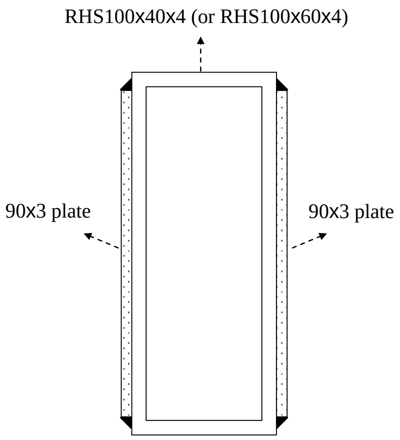

Fig. 1 Reinforced RHS cross sections

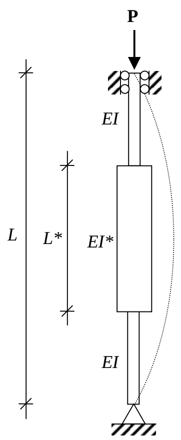

Fig. 2 Partial reinforcement of slender test specimens

RHS members were concentrically loaded in compression to failure. To investigate the effect of the member slenderness ratio on effectiveness of the reinforcement, two sets of test specimens were prepared from two unreinforced sections: RHS 100×40×4 mm and RHS100×60×4 mm. Test specimens were reinforced by welding 3-mm-thick steel plates with four different length ratios: 0.25, 0.50, 0.75 and 0.975. Test results were compared with the analytical results for elastic buckling and a simple design expression was proposed to predict the compressive strength of steel RHS members reinforced along part of their length with welded steel plates by modifying the provisions of AISC 360-10 (2010) to account for the partial reinforcement.

2. Experimental study

A total of 28 (6 *unreinforced* and 22 *partially-reinforced*) slender steel compression members were tested under monotonically increasing concentric load. Half of the test specimens were cut from RHS100×40×4 mm members and the other half from RHS100×60×4 mm members. Due to the height limitations of the test setup, the length of the test specimens was fixed to L=2 m. Thus, the *slenderness ratios* for the *reference (unreinforced)* specimens are KL/r=125 for the RHS100×40×4 and KL/r=83 for the RHS100×60×4 sections. *Partially-reinforced* test specimens were prepared by welding 90×3 mm steel plates to their larger sides, as schematically shown in Fig. 1 in cross section. The length of the reinforcing plates (L^*=0.5, 1.0, 1.5 or 1.95 m) was deliberately selected to be smaller than the length of the specimens to produce *partially reinforced* test specimens, schematically illustrated in Fig. 2, where EI^* and EI are minor-axis flexural rigidities of the *reinforced* and *unreinforced* sections, respectively. In addition to slender-column tests, a total of 14 stub-column tests were conducted to determine material properties of the slender test specimens under compression.

2.1 Stub-column tests

Since compressive behavior of a steel member highly depends on the residual stresses stored in the member during its manufacture, the basic mechanical properties of a compression member are typically obtained from stub-column tests, instead of coupon tests (Nagaraja Rao and Tall 1962, Shaat and Fam 2009). Stub-column (SC) tests were performed on 200-mm-long specimens cut from the original test specimens. In addition to *unreinforced (reference)* SC specimens, *reinforced* SC specimens were cut from the reinforced portions of the *partially-reinforced* test specimens. Conducted with an aim to determine the compressive behavior of members reinforced along their entire length in the absence of slenderness effects, the test results of the *reinforced* SC specimens are assumed to provide upper limits for the slender *partially-reinforced* test specimens. In addition, to investigate the possible effects of welding applied during the reinforcement stage of the slender test specimens, "*subsequently-unreinforced*" SC specimens were obtained from *reinforced* SC specimens by removing the welded plates with special care so as not to damage the resulting specimens. At least two specimens were tested in each set. Thus, in this stage of the study, in 6 sets, a total of 14 (5 *unreinforced*, 5 *fully-reinforced* and 4 *subsequently-unreinforced*) SC specimens were tested. The number and names of the SC specimens in each set are listed in Table 1.

SC specimens were named in SCXXPX-X pattern (see Table 1). The first two numbers after the letters SC (which can be either 40 or 60) indicates the smaller dimension (width) of the cross section in mm, the number after the letter P can be 0 or 3 with 0 meaning no reinforcing plate (reference specimen) and 3 meaning a reinforced specimen with 3-mm-thick plates, and the number after the hyphen (which can be 1, 2 or 3) gives the number of the specimen tested in the set. As an example, the specimen SC40P0-1 is the first *unreinforced* SC specimen with RHS100×40×4 section, SC60P3-2 is the second *reinforced* SC specimen composed of 90×3 mm steel plates welded to a RHS100×60×4 section (see Fig. 1). The *subsequently-unreinforced* specimens have a * symbol before the hypen. For example, SC60P3*-1 is the first *subsequently-unreinforced* SC specimen prepared by removing the reinforcing plates of a SC specimen with the same geometrical and material properties as SC60P3 specimens.

The SC specimens were tested in Materials Laboratory

Table 1 Summary of main test results for stub-column specimens

Test Set	Specimen Name		E_{SC} (GPa)	$F_{y,SC}$ (MPa)	$F_{u,SC}$ (MPa)
SC40P0	SC40P0-1		183.4	324	367.0
	SC40P0-2		185.6	348	360.5
		Average	*184.5*	*336*	*363.7*
SC40P3*	SC40P3*-1		187.2	352	358.8
	SC40P3*-2		172.1	354	362.4
		Average	*179.7*	*353*	*360.6*
		Ratio to SC40P0	*0.97*	*1.05*	*0.99*
SC40P3	SC40P3-1		184.0	326	368.0
	SC40P3-2		190.3	306	368.8
		Average	*187.2*	*316*	*368.4*
		Ratio to SC40P0	*1.01*	*0.94*	*1.01*
SC60P0	SC60P0-1		193.3	345	371.8
	SC60P0-2		187.8	354	383.5
	SC60P0-3		189.7	347	380.7
		Average	*190.3*	*349*	*378.6*
SC60P3*	SC60P3*-1		185.6	309	374.8
	SC60P3*-2		183.9	330	368.5
		Average	*184.7*	*320*	*371.6*
		Ratio to SC60P0	*0.97*	*0.92*	*0.98*
SC60P3	SC60P3-1		189.0	335	358.6
	SC60P3-2		180.2	362	363.4
	SC60P3-3		184.1	328	358.6
		Average	*184.4*	*342*	*360.2*
		Ratio to SC60P0	*0.97*	*0.98*	*0.95*

of Civil Engineering Department at Kocaeli University using the testing machine shown in Fig. 3(a). The load was recorded using a load cell (Fig. 3(b)) with a capacity of 100 tons. The longitudinal strains on the specimens were measured using strain gages placed at mid-height, at the middle of each side of the members, as shown in Fig. 3(b). Thus, four strain gage measurements were taken during the tests of each SC specimens. Strain gages were attached directly to the reinforcing plates on the reinforced SC specimens.

2.2 Member tests

Partially-reinforced specimens, cut from either RHS100×40×4 or RHS100×60×4 members, were prepared by welding steel plates of a predefined length, 0.5, 1.0, 1.5 or 1.95 m, which correspond to the *reinforcement length ratios* (defined as L^*/L ratios, see Fig. 2) of 0.25, 0.50, 0.75 and 0.975, respectively. To simulate a possible real retrofitting case where the ends of the members may not be easily accessible, *nearly-fully reinforced* specimens were prepared using steel plates cut 25 mm shorter than the length of the test specimens in each end (i.e., L^*=1950 mm). Since all specimens were reinforced by using 3 mm× 90 mm steel plates, the *flexural rigidity ratios* (defined as

(a) Test machine

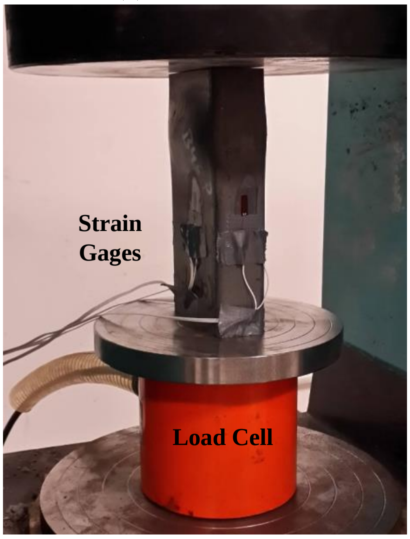

(b) Loading and measurement system

Fig. 3 Test setup for stub-column specimens

EI^*/EI ratios) are 1.94 for 40-mm wide specimens and 1.79 for 60-mm wide specimens for minor-axis flexural buckling, which was the governing limit state for all test specimens. To obtain reliable average of the test results, most sets included three test specimens. Only two sets, from which the SC specimens were cut, contain two specimens.

Slender test specimens were named, following a similar convention to SC specimens, in BXXPXLX-X pattern (Table 2). The first two numbers after the letter B indicate the width (in mm) of the cross section, the number after the letter P can be 0 or 3 with 0 meaning an unreinforced specimen and 3 meaning a *reinforced* specimen with 3-mm-thick plates and the number after the letter L gives information about the length of the reinforcing plates: the numbers 0, 1, 2, 3 and 4 correspond, respectively, to the reinforcement length ratios of 0, 0.25, 0.50, 0.75 and 0.975. Finally, the number after the hyphen (which can be 1, 2 or 3) gives the number of the specimen tested in the set. As an example, the specimen B40P0L0-1 is the first *reference (unreinforced)* specimen with RHS100×40×4 section, B60P3L2-3 is the third specimen in the test set in which the

Table 2 Summary of main test results for slender test specimens

Specimen Name	δ (mm)	L/δ			P_{max} (kN)	k_v (kN/mm)
B40P0L0-1	1.65	1212	*		108.5	59.4
B40P0L0-2	0.89	2254			91.2	68.3
B40P0L0-3	0.60	3333			113.5	75.9
				Average	*104.4*	*67.9*
B40P3L1-1	2.26	884	*		133.5	82.2
B40P3L1-2	2.83	708	*		109.6	67.2
B40P3L1-3	1.74	1151	*		127.9	80.2
				Average	*123.7*	*76.5*
				% Gain	*18.5*	*12.7*
B40P3L2-1	3.24	618	*		131.3	83.1
B40P3L2-2	2.90	690	*		140.2	82.7
B40P3L2-3	1.00	2000			166.9	98.2
				Average	*146.1*	*88.0*
				% Gain	*40.0*	*29.6*
B40P3L3-1	2.00	1000	*		187.4	104.0
B40P3L3-2	0.40	5000			183.6	103.7
				Average	*185.5*	*103.9*
				% Gain	*77.7*	*53.0*
B40P3L4-1	0.41	4848			17.4	105.0
B40P3L4-2	5.51	363	*		139.6	81.9
B40P3L4-3	3.26	613	*		160.9	92.0
				Average	*157.6*	*93.0*
				% Gain	*51.0*	*36.9*
B60P0L0-1	0.34	5818			229.2	98.0
B60P0L0-2	0.33	6154			234.2	104.1
B60P0L0-3	0.55	3636			212.5	104.9
				Average	*225.3*	*102.3*
B60P3L1-1	1.18	1702			283.1	121.2
B60P3L1-2	1.36	1468	*		287.5	120.8
B60P3L1-3	0.98	2051			273.6	122.3
				Average	*281.4*	*121.4*
				% Gain	*24.9*	*18.7*
B60P3L2-1	1.10	1798			292.0	122.3
B60P3L2-2	0.73	2759			288.1	125.8
B60P3L2-3	1.38	1455	*		269.8	116.1
				Average	*283.3*	*121.4*
				% Gain	*25.8*	*18.6*
B60P3L3-2	0.70	2857			361.5	125.0
B60P3L3-3	1.36	1468	*		340.9	125.6
				Average	*351.2*	*125.3*
				% Gain	*55.9*	*22.4*
B60P3L4-1	0.90	2222			309.3	132.5
B60P3L4-2	0.50	4000			376.0	141.6
B60P3L4-3	0.53	3810			378.8	132.1
				Average	*354.7*	*135.4*
				% Gain	*57.4*	*32.3*

specimens with unreinforced cross section of RHS100×60×4 was *reinforced* by welding 3-mm thick steel plates in 1-m length. It is to be noted that SC40 specimens were cut

(a) Test frame

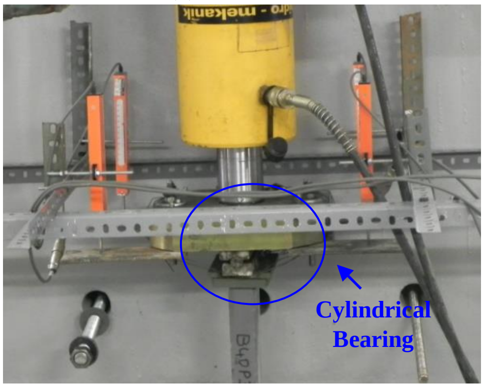

(b) LVDTs for measuring vertical displacement of the specimen end

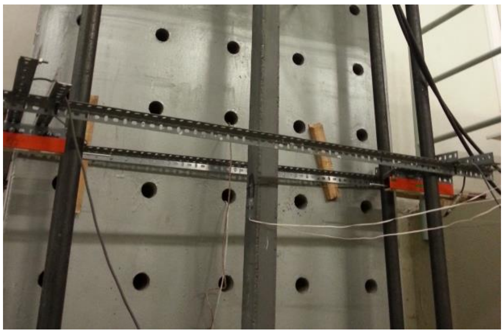

(c) LVDTs for measuring horizontal displacement of the specimen at mid-height

Fig. 4 Test setup for slender test members

from B40P3L3-3 and SC60 specimens were cut from B60P3L3-1 test specimens; for this reason, only two specimens were tested in B40P3L3 and B60P3L3 test sets.

Since initial out-of-straightness can greatly affect buckling behavior of a compression member and since welding applied during the reinforcing stage may change the out-of-straightness pattern of the reinforced specimens significantly, the mid-height values of the initial out-of-straightness (δ) of the test specimens in the plane of buckling were measured using a laser optical displacement sensor before the specimens were loaded to failure. The measured values of δ as well as the L/δ ratios for all test specimens are listed in Table 2, which indicates that the δ/L values of all *unreinforced* members were considerably small, with the maximum value being 1/1212. Table 2 also shows that the δ/L values of B40 specimens were, in general, larger than those of B60 specimens in similar sets. The largest δ/L value recorded among B60P3 specimens was 1/1455 while in B40P3 specimens it was 1/363. However, only one B40P3 specimen has a value larger than the maximum tolerance specified in the AISC Code of Standard Practice, as stated by AISC 360-10 (2010), for uniform members: 1/500. The slender column specimens with initial out of straightness greater than L/1500, which is the value used in the development of AISC column curves, are marked in Table 2 with a star (*) symbol in the fifth column.

Slender test specimens were tested in Structural Mechanics Laboratory of Civil Engineering Department at Kocaeli University using a test setup shown in Fig. 4(a). To ensure minor-axis buckling, lubricated cylindrical bearings (see Fig. 4(b)) were placed at the ends of the specimens. These supports were designed to behave as pinned supports in minor-axis buckling whereas as nearly-fixed supports in major-axis buckling. The compressive load was applied to the specimens through a hydraulic jack (with 100 ton capacity) placed at the top of the upper support. The compression load was measured using a pressure gage. Vertical displacement of the upper end of each specimen was measured using four linear variable differential transformers (LVDTs) placed on four corners of the moving head as shown in Fig. 4(b).

The lateral deflection at mid-height of each specimen was measured using two LVDTs (see Fig. 4(c)). The longitudinal strains at mid-height of the specimens were measured using two strain gages attached to the outermost fibers in the central cross section (Fig. 5).

3. Test results and discussion

3.1 Stub-column tests

The stub-column (SC) stress-strain curves plotted using the average values of strain measurements taken from four sides of SC specimens are presented in Fig. 6. The main test results, namely, stub-column elasticity modulus (E_{SC}), defined as the slope of the linear portion of the SC stress-strain curves, stub-column yield strength ($F_{y,SC}$), which equals to the 0.2% offset yield strength obtained from SC curves, and stub-column ultimate compressive strength ($F_{u,SC}$), which corresponds to the peak value of the SC curves are presented in Table 1.

Fig. 5 Strain gages attached to the outermost fibers at the central cross section

As it can be inferred from Fig. 6, all *unreinforced* SC specimens yielded before the onset of web local buckling, which resulted in noticeable strength loss causing the "failure" of the specimens (see also Fig. 7(a)). The gradual transition from linear elastic behavior to yield plateau shows the existence of built-in residual stresses in *cold-formed* tube sections. The average values of yield strengths (see Table 1) are approximately 336 and 349 MPa for RHS100×40×4 and RHS100×60×4 sections, respectively. Similarly, the average values of elasticity modulus are approximately 185 and 190 GPa for the same RHS sections. The listed values in Table 1 show very little variation between tests in the same set. It can also be noted from Table 1 that the average stub-column compressive strength of each section is approximately 30 MPa greater than its average yield stress.

The fact that local buckling occurred after yielding in all reference specimens indicates that none of the tested tubular sections contain slender element. AISC 360-10 (2010) classifies RHS sections under uniform compression as a non-slender element section if the flat width-to-thickness ratio of its any compression element is smaller than the limiting value $\lambda_r = 1.4\sqrt{E/F_y}$, where E is the modulus of elasticity and F_y is the yield strength of the steel.

Using the stub-column test results for material properties, λ_r=32.8 for RHS100×40×4 and λ_r=32.7 for RHS100×60×4 section. Since the webs of both sections have equal length (100 mm), the maximum width-to-thickness ratios for the unreinforced sections can be calculated as 25 even when the outside dimensions are used. Thus, as per AISC 360-10, neither of the tested RHS cross section contains a non-slender element, which is consistent with the test results.

The effects of welding on the compressive behavior of SC40 specimens can be studied by plotting stress-strain curves of SC40P0 and SC40P3* specimens in the same graph as shown in Fig. 8(a). A similar graph is plotted in Fig. 8(b) for SC60 specimens. The graphs presented in Fig. 8 show that welding does not cause noticeable decrease in the compressive strength of any *reinforced* SC specimen.

The average decrease in ultimate strength is only 1% in SC40 specimens and 2% in SC60 specimens. Similarly, as far as the average yield strength is concerned, welding appears to have no adverse effect on the compressive behavior of SC40 specimens; instead, a 5% increase in average yield strength is observed. On the other hand, the average yield strength of the SC60P3* specimens is 8% smaller than that of SC60P0 specimens. As shown in Fig. 8(b), the stress-strain curves of SC60P3* specimens begin to deviate from linearity at much smaller stresses than the other specimens in the same graph, which is believed to be

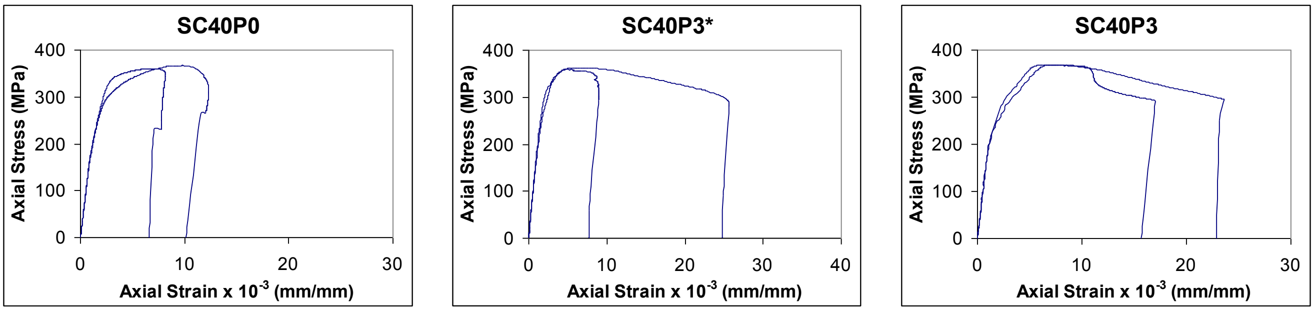

(a) SC40 specimens

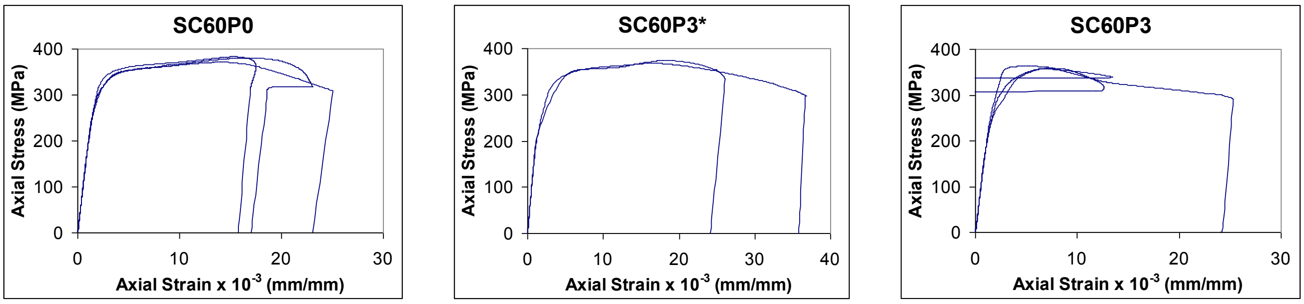

(b) SC60 specimens

Fig. 6 Axial stress-strain plots for stub-column specimens

(a) Unreinforced SC40 (left) and SC60 (right) specimens

(b) Reinforced SC40 (left) and SC60 (right) specimens

(c) Subsequently unreinforced SC40 (left) and SC60 (right) specimens

Fig. 7 Failure of stub-column specimens due to excessive local buckling

the main reason for such a decrease in the offset yield strength.

The effect of reinforcement on the compressive behavior of the SC specimens can be assessed from Table 1. The average ultimate compressive strength is 368 MPa for SC40P3 specimens and 360 MPa for SC60P3 specimens. Similarly, the average values of the elasticity modulus are approximately 187 and 184 GPa, respectively. These results show the effectiveness of steel-reinforcement on stub-column behavior of RHS tubes. It is to be noted that reinforcing SC specimens using 90×3 mm steel plates causes considerable increase (53% for SC40 and 46% for SC60 specimens) in the cross sectional area of both built-up sections. The behavior of the *reinforced* SC specimens can be studied more thoroughly by plotting the stress-strain curves of *reinforced* SC40 and SC60 specimens compared to those of their *unreinforced* counterparts, presented in Fig. 9. Average compressive strength of SC40P3 specimens is almost the same as that of SC40P0 specimens. On the other hand, the axial stress-strain curves of SC40P3 specimens deviate from linearity at smaller stresses, which results in 6% decrease in average yield strength in these specimens compared to SC40P0 specimens. As shown in Fig. 9(b), in pre-yielding stage, two of the three SC60P3 specimens exhibit almost the same behavior as SC40P3 specimens. The compressive behavior of SC60P3 specimens differs from that of SC40P3 specimens mainly in that they cannot reach the maximum stress attained by their reference specimens. The average compressive strength of SC60P3 specimens is 5% smaller than that of SC60P0 specimens. From Fig. 9(a) and Table 1, it can also be noticed that the effect of reinforcement on stub-column elasticity modulus

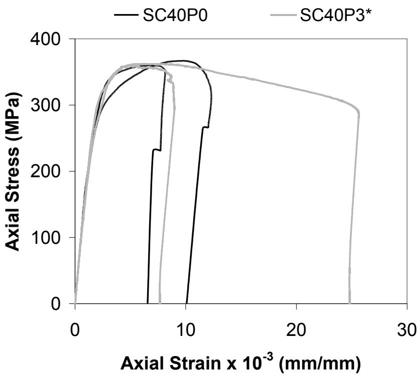

(a) SC40 specimens

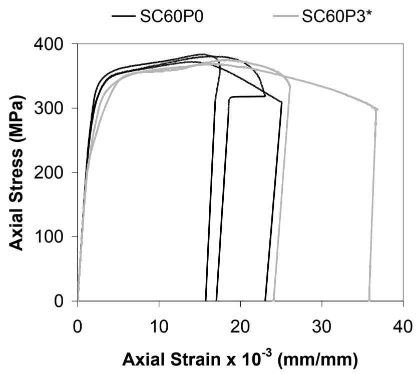

(b) SC60 specimens

Fig. 8 The effect of welding on compressive behavior of stub-column specimens

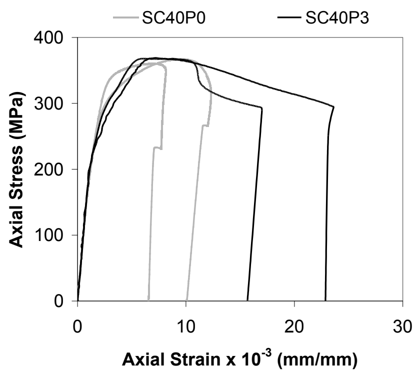

(a) SC40specimens

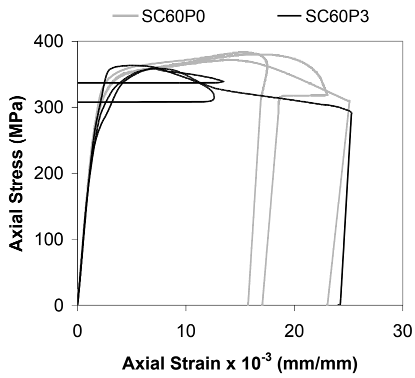

(b) SC60specimens

Fig. 9 The effect of reinforcement on compressive behavior of stub-column specimens

Fig. 10 Local buckling of larger side walls in SC specimens

is not greater than 3% in any *reinforced* SC specimens.

Similar to the *unreinforced* SC specimens, all *reinforced* SC specimens failed due to web local buckling (see Fig. 7(b)) and none of the *reinforced* specimens were subjected to connection failure. When the *reinforced* specimens were examined after the tests, it was observed that both the reinforcing plates and the sidewalls of the tubes were subjected to local buckling (Fig. 10). It is believed that buckling of each component (plate and tube walls) did not occur, in general, simultaneously and in the same direction. As shown in Fig. 5, in most of the reinforced specimens, two abrupt changes can be observed in the slope of the stress-strain curve before the yielding plateau. Each change is believed to occur due to the initiation of yielding and/or local buckling in one component (plate or tube walls).

3.2 Member tests

The main test results, namely axial load capacity (P_{max}) and elastic axial stiffness (k_v), defined as the slope of the linear part of the axial load versus axial displacement curve, for slender test specimens are summarized in Table 2, which also presents the average values of the test results for each set. Percent increases in axial capacity and stiffness for the *reinforced* members, as compared to their *unreinforced* counterparts, are also presented in the table. Table 2 shows that the average percent increases in axial capacities of B40P3 specimens are 19, 40, 78 and 51% for the length ratios of 0.25, 0.50, 0.75 and 0.975 (i.e., for L1, L2, L3 and L4 specimens), respectively. The corresponding values for B60P3 specimens are 25, 26, 56 and 58%, respectively. Similarly, the percent increases in axial stiffness are approximately 13, 30, 53 and 37% for B40P3 specimens and 19, 19, 22 and 32% for B60P3 specimens, for the same length ratios. In general, increase in stiffness is smaller than increase in strength for all specimens

Increase in strength for *partially-reinforced* specimens can be attributed to decrease in slenderness ratios. The slenderness ratio of B40P3 specimens decreases theoretically from 125 to 110 as the reinforcement length ratio increases from 0 to 1. This decrease is smaller in B60P3 specimens, from 83 to 75. Surely, decrease in slenderness ratio is related to increase in minor-axis moment of inertia due to the addition of the reinforcing plates. Reinforcing an RHS100×40×4 section using 90×3 mm plates causes 94% increase in their minor-axis moment of inertia. Corresponding increase in moment of inertia is 78% in B60P3 specimens. Increase in elastic axial stiffness, on the other hand, can typically be attributed to the increase in cross sectional area due to the addition of the reinforcing plates. As mentioned previously, reinforcing B40 specimens using 3-mm thick plates results in 53% increase in the cross sectional area at the reinforced sections. Similarly, increase in the cross sectional area in B60P3 specimens is 46%.

The compressive behavior of the *partially-reinforced* specimens can be studied more thoroughly from Figs. 11-13. Fig. 11 shows the deformed (buckled) shapes of the slender test specimens. The graphs given in Fig. 12(a) plot the axial load (in vertical axis) versus the longitudinal strains (in horizontal axis) at the outermost fibers in the central cross section of B40 specimens at mid-height. Similarly, the graphs in Figs. 12(b) and (c) plot the variation of vertical displacement (in horizontal axis) and mid-height lateral displacement (in horizontal axis), respectively, as a function of applied load (in vertical axis). Similar graphs are presented for B60 specimens in Fig. 13. Due to some technical problems, unloading curves of six test specimens cannot be recorded during the tests. Typical failure modes for the slender test specimens are presented in Fig. 14.

All *unreinforced* specimens failed due to excessive overall buckling. The deformed shapes for *unreinforced* specimens were symmetrical and close to the Euler's sinusoidal shape (see Figs. 11(a),(f)). B40P0L0-2 and B60P0L0-3 specimens were observed to start bending (buckling) at smaller load levels, while the other reference specimens remained almost straight until the applied load was close to the axial load capacity. This can also be observed from the load-strain curves given in Figs. 12(a) and 13(a). The strain gage measurements taken from the inner and outer faces of B40P0L0-2 and B60P0L0-3 specimens start to deviate at smaller load levels. This can be attributed to the presence of relatively large initial out-of-straightness and/or accidental eccentricity of the load.

Overall buckling was also observed in the *partially-reinforced* specimens; however, full-length buckling was, in general, followed by "localized" buckling observed at either top or bottom unreinforced segment of the specimen as shown in Fig. 14(a). In this failure mode, the deformed shapes of the specimens were usually not symmetric about the mid-height (Figs. 11(b)-(e) and Fig. 11(g)-(j)). In some cases, local buckling and yielding were also observed at the section where the cross section changed abruptly, as shown in Fig. 14(b).

Figs. 12 and 13 reveal that, among the specimens tested in the same set, the compressive strength of the specimens which remained straight for a long time and buckled abruptly, i.e., the specimens whose strain gage measurements taken from the inner and outer faces start to deviate at larger load levels, is larger than that of the specimens which started to bend at smaller load levels and buckled gradually. This result can again be attributed to the presence of relatively large out-of-straightness and/or accidental load eccentricity. In fact, the axial capacities of the "starred" specimens in Table 2 (which have initial mid-height out-of-straightness larger than $L/1500$) are usually less than that of an "unstarred" specimen in the same set.

Figs. 12 and 13 also show that, as expected, the average compressive strength and stiffness of the *partially-reinforced* B40 specimens increases as the reinforcement length ratio increases from 0.25 to 0.75. On the other hand, contrary to the expectations, the strength and stiffness of B40P3L4 specimens are less than those of B40P3L3 specimens, which means that reinforcing the B40 columns along the near full length was not as effective as reinforcing them along only in their 3/4 length. Similarly, the average compressive strength of B60P3L4 specimens is almost equal to that of B60P3L3 specimens. The unexpected strength loss observed in *"nearly-fully" reinforced* specimens can be attributed to the premature failure of some of the test specimens in these sets due to excessive yielding (bearing failure) taking place on their unreinforced ends. When combined with the adverse effect of the existence of relatively large initial out-of-straightness in two of the B40P3L4 specimens, the premature bearing failure is believed to result in 15% decrease in average strength in *nearly-fully reinforced* B40 specimens compared to the B40 specimens reinforced along their 3/4 length.

3.3 Proposed design expression

AISC 360-10 (2010) defines nominal compressive strength P_n for a uniform steel member with subject to axial compression through the centroidal axis as the lowest value obtained based on the applicable limit states of flexural, torsional, flexural-torsional buckling and local buckling. According to the User Note E1.1 in the specification, for rectangular hollow sections without slender elements, it is sufficient to compute P_n based only on the limit state of flexural buckling. Thus, the nominal compressive strength of a non-slender element steel RHS column can be determined from

$$P_n = F_{cr} A_g \tag{1}$$

where A_g is the gross cross sectional area of the steel section and F_{cr} is the critical stress which can be determined, depending on the slenderness of the member (KL/r), from:

$$\begin{aligned} F_{cr} &= \left[0.658^{F_y/F_e}\right] F_y \quad \text{when} \quad \frac{KL}{r} \le 4.71\sqrt{\frac{E}{F_y}}, \\ F_{cr} &= 0.877 F_e \quad \text{when} \quad \frac{KL}{r} \ge 4.71\sqrt{\frac{E}{F_y}} \end{aligned} \tag{2}$$

where F_y is the yield stress; F_e is the elastic buckling stress, which can be determined, as a function of modulus of elasticity E and member slenderness ratio, by the following equation

$$F_e = \frac{\pi^2 E}{\left(KL/r\right)^2} \tag{3}$$

For unreinforced test specimens with RHS100×40×3 section (KL/r=125), using stub-column material properties

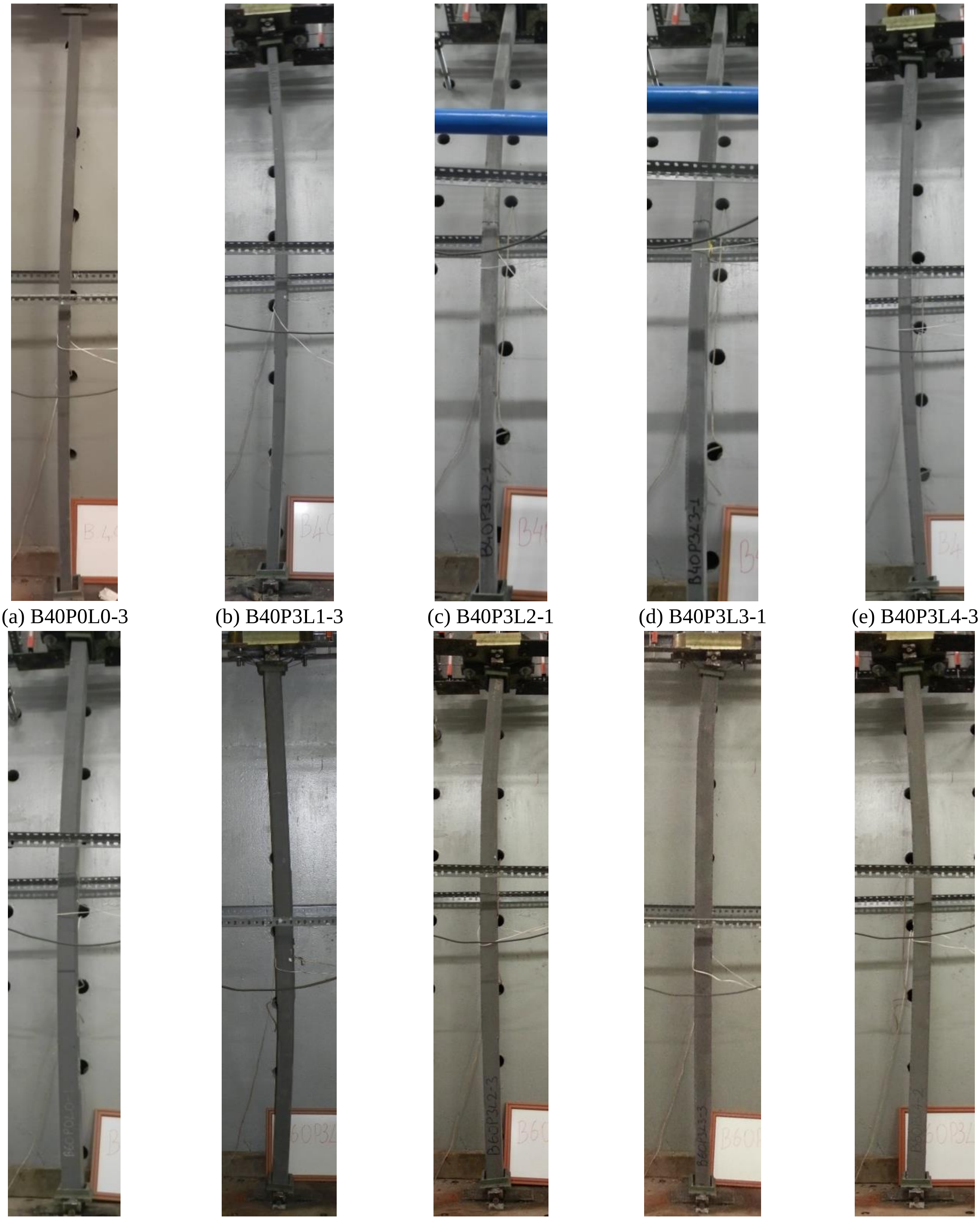

(a) B40P0L0-3 (b) B40P3L1-3 (c) B40P3L2-1 (d) B40P3L3-1 (e) B40P3L4-3

(f) B60P0L0-1 (g) B60P3L1-1 (h) B60P3L2-3 (i) B60P3L3-3 (j) B60P3L4-2

Fig. 11 Typical buckled shapes of slender test specimens

(E_{SC}=184.5 GPa and $F_{y,SC}$=336 MPa), the nominal compressive strength can be computed using the elastic buckling expression in Eq. (2) as P_n=106.6 kN. The average compressive strength of B40P0L0 specimens, 104.4 kN (Table 2), differs from the computed nominal value only 2%.

Since AISC provisions are defined only for uniform members, the design expressions given in Eqs. (1)-(2) cannot directly be used for the *partially-reinforced* test specimens. However, with an aim to provide an upper limit for the compressive strength of the *partially-reinforced* specimens, these equations can be used to compute the

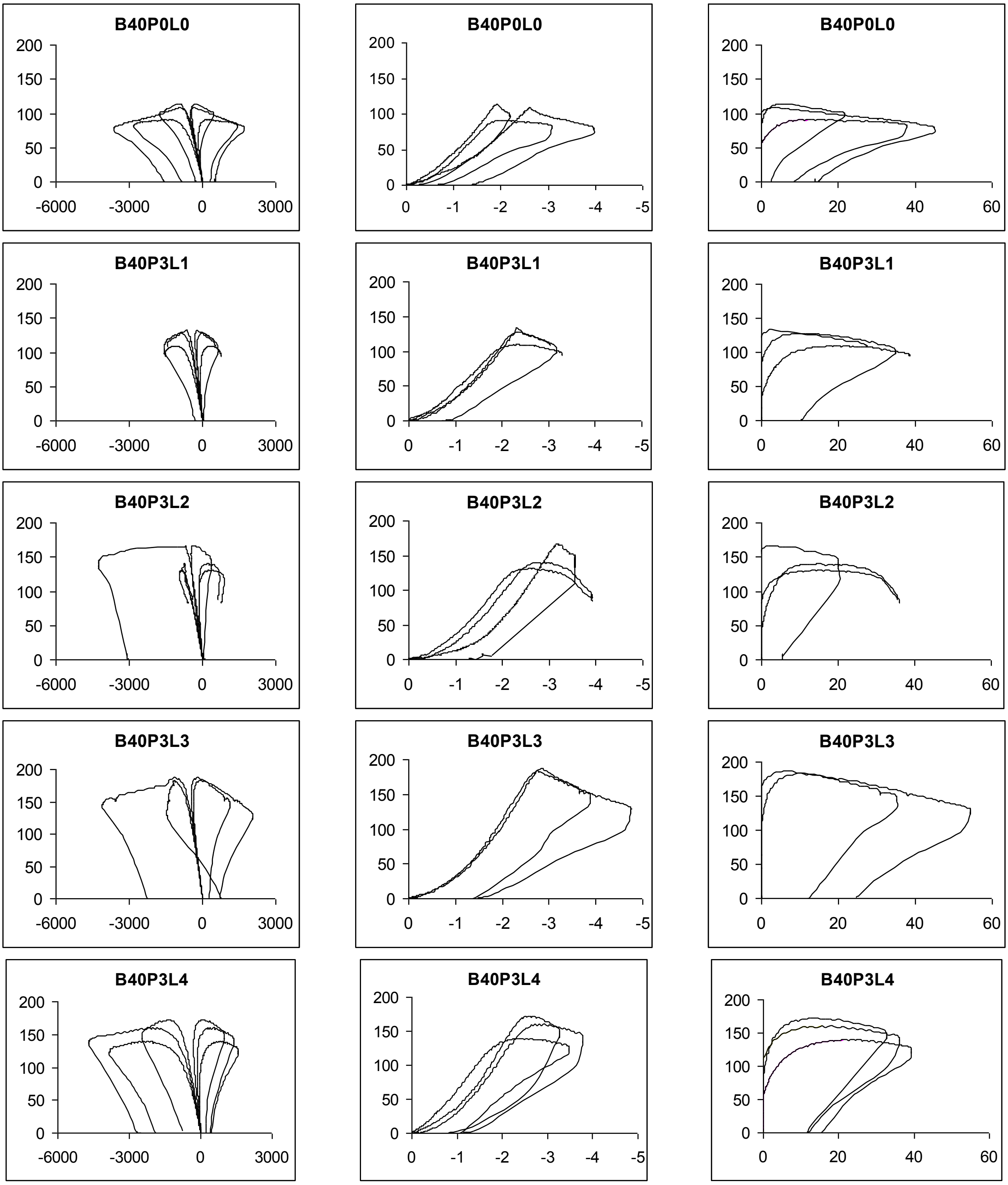

(a) Axial strain (mm/m) versus axial load (kN)

(b) Axial displacement (mm) versus axial load (kN)

(c) Mid-height lateral displacement (mm) versus axial load (kN)

Fig. 12 Variation of (a) axial strain, (b) axial displacement and (c) mid-height lateral displacement (in horizontal axes) as a function of applied axial load (in vertical axes) for B40 specimens

nominal compressive strength of the *"fully-reinforced"* members (i.e., the members with $L^*=L$). In this case, the main problem is the use of the appropriate material properties (E and F_y) for the composite section formed by welding hot-rolled steel plates to a cold-formed steel tube. It is believed that the mechanical properties determined from the *reinforced* stub-column specimens can be used to calculate the nominal strength of the *fully-reinforced* slender columns. Thus, using the mechanical properties of SC40P3 specimens (E_{SC}=187.2 GPa and $F_{y,SC}$=316 MPa),

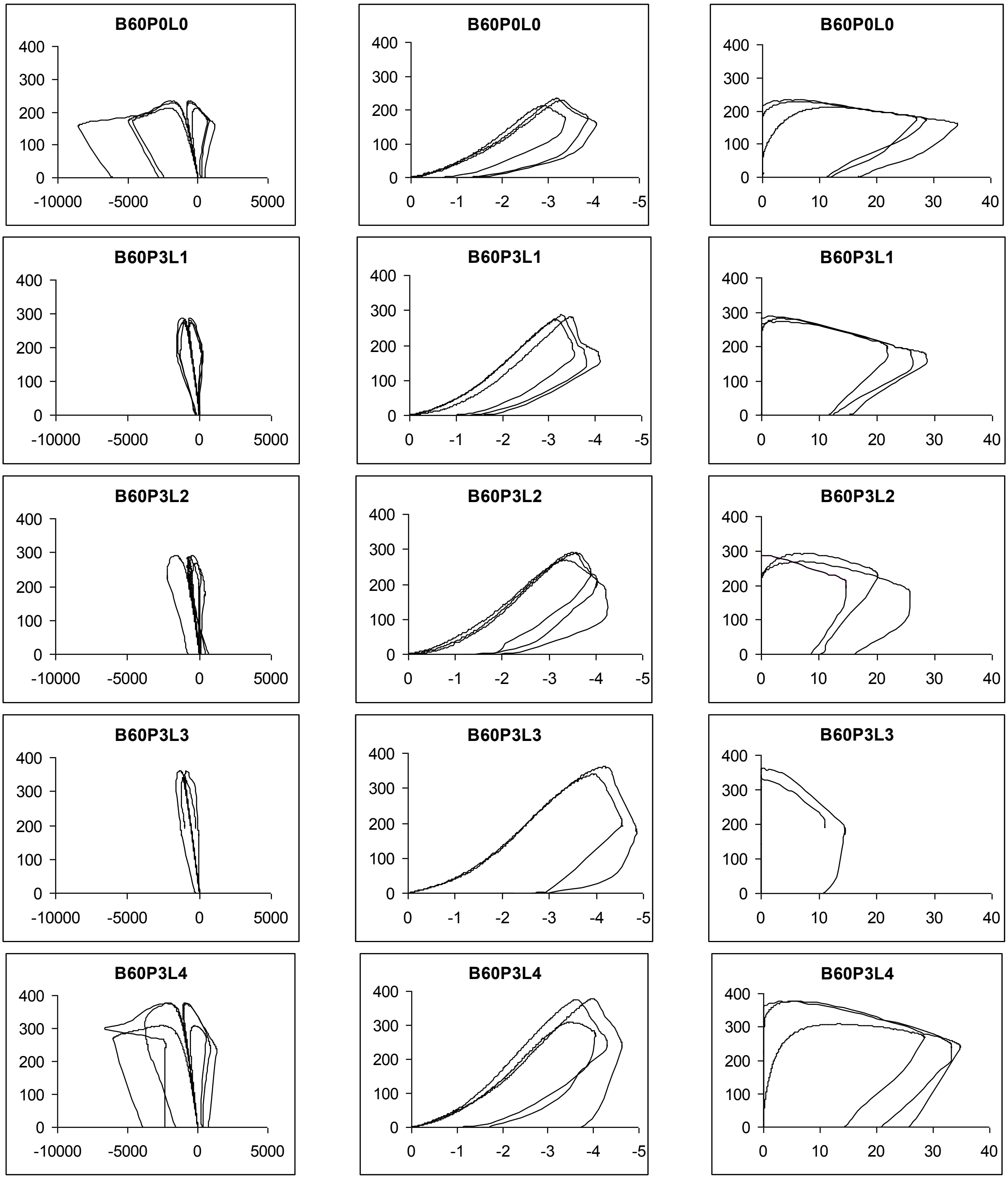

(a) Axial strain (mm/m) versus axial load (kN)

(b) Axial displacement (mm) versus axial load (kN)

(c) Mid-height lateral displacement (mm) versus axial load (kN)

Fig. 13 Variation of (a) axial strain, (b) axial displacement and (c) mid-height lateral displacement (in horizontal axes) as a function of applied axial load (in vertical axes) for B60 specimens

the nominal compressive strength of a 2-m long, pin-ended member with RHS100×40×3 section reinforced along its full length using 3-mm thick welded steel plates (as shown in Fig. 1), which has a member slenderness ratio of KL/r=109.5, can be computed using Eq. (2) as 207.6 kN. This means that the strength of a column with RHS100×40×3 section can be increased by 95% when the column is *fully reinforced*. Unfortunately, *fully-reinforced* specimens (L^*=L) were not tested in the experimental program and some of the *nearly-fully reinforced* B40

(a) Buckling of unreinforced segments

(b) Local buckling at the end of the reinforced region

Fig. 14 Typical failure modes for slender test specimens

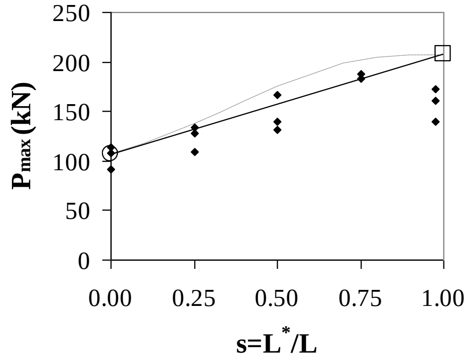

(a) B40P3 specimens

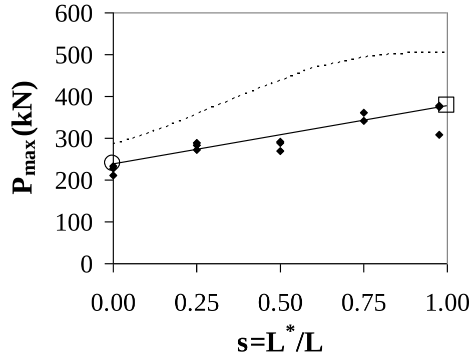

(b) B60P3 specimens

(Note: In the graphs; *filled bullets*: test data; *circular bullets*: $P_{n,s=0}$ (nominal compressive strength of unreinforced RHS member as per AISC360-10; *square bullets*: $P_{n,s=1}$ (nominal compressive strength of fully-reinforced RHS member as per AISC360-10; *dashed line*: $0.877P_e$ (where P_e is elastic buckling load for the stepped member); *solid line*: predictions of the proposed design equation (Eq. (4))

Fig. 15 Linear design equation proposed for the prediction of nominal compressive strength of partially-reinforced RHS members

specimens (L*=0.975L) were observed to fail prematurely due to the end complications. On the other hand, one can see that the average strength of 3/4-length-reinforced specimens (185.5 kN) is reasonably close to this limit strength.

As far as the design of the *partially-reinforced* members is concerned, the basic problem is the change of cross sectional properties (area, moment of inertia, radius of gyration) along the *stepped* member. AISC provisions given in Eqs. (1)-(3) require the calculation of stresses, which are no longer constant through the length of the member. Using analytical methods available in literature, *elastic* buckling load, or Euler load, (P_e) can directly be computed as illustrated in Pinarbasi Cuhadaroglu *et al*. (2012). However, the Euler load can only be used when the buckling is *elastic*. If the column is sufficiently slender (which is also difficult to define in stepped members) to buckle elastically, its nominal compressive strength may be computed from P_n=0.877P_e, which takes into consideration the initial-out-of straightness of the member. With an aim to provide an upper limit for the nominal strength, the elastic buckling loads for the 40-mm wide test specimens were computed using the analytical method presented in Pinarbasi Cuhadaroglu *et al*. (2012) with E=E_{SC40P0}=184.5 GPa. Accordingly, the *elastic* buckling load (P_e) for the B40 specimens are 121.5, 156.5, 199.4, 229.8, 235.3 and 235.4 kN for the reinforcement length ratios of s=L*/L=0, 0.25, 0.5, 0.75, 0.975 and 1.0. After multiplying with 0.877, these values are plotted in Fig. 15(a) with a dashed line. The nominal compressive strengths of the *unreinforced* and *fully-reinforced* specimens computed using AISC360-10, as well as the test data, are also added to the same graph using a circular bullet, square bullet and filled bullets, respectively. The premature failure of B40P3L4 specimens is more apparent from Fig. 15(a). The experimentally-determined strengths of the other *partially-reinforced* specimens are very close and always smaller than the nominal elastic buckling load (0.877P_e).

A simple and conservative linear equation shown in Fig. 15(a) with a solid line can be proposed for the prediction of the compressive strengths of the test specimens. The proposed design expression simply requires computing the nominal compressive strengths of the *unreinforced* and *fully-reinforced* specimens using the provisions defined in ANSI/AISC 360-10 (2010) and making linear interpolation between them to account for the partial reinforcement of the specimen, which can be formulated as follows

$$P_{n,s} = P_{n,s=0} + s\left(P_{n,s=1} - P_{n,s=0}\right) \tag{4}$$

where $P_{n,s}$ is the nominal compressive strength of a *partially-reinforced* steel member, $P_{n,s=0}$ and $P_{n,s=1}$ are the nominal compressive strengths of the corresponding *unreinforced* and *fully-reinforced* steel members computed from AISC provisions given in Eqs. (1)-(3) using the appropriate stub-column properties and s is the ratio of the length of the reinforcing plates to the length of the member (i.e., the reinforcement length ratio; $s=L^*/L$, see Fig. 2).

Similar computations can be done for the test specimens with 60-mm wide tubes. Using stub-column mechanical properties (E_{SC60P0}=190.3 GPa and $F_{y,SC60P0}$=349 MPa), the nominal compressive strength of the *unreinforced* test specimens with RHS100×60×3 section (KL/r=83.3) can be computed as $P_{n,s=0}$=240.2 kN. The average compressive strength of the B60P0L0 specimens, 225.3 kN (Table 2), differs from the nominal value only 7%. Similarly, using the mechanical properties obtained from the tests of SC60P3 specimens (E_{SC60P3}=184.4 GPa and $F_{y,SC60P3}$=341.7 MPa), the nominal compressive strength of a 2-m long, pin-ended column with RHS100×60×3 section reinforced in full-length using 3 mm welded steel plates (with a slenderness ratio of KL/r=74.8) can be computed as $P_{n,s=1}$=376.7 kN, which means that the strength of the column can be increased 57% provided that it is reinforced in full-length. Again, using the analytical method given in Pinarbasi Cuhadaroglu *et al*. (2012), the elastic buckling loads (P_e) for the 60-mm wide *partially-reinforced* test specimens are determined as 322.1, 402.6, 499.0, 562.2, 573.3 and 573.5 kN for the reinforcement length ratios of $s=L^*/L$=0, 0.25, 0.5, 0.75, 0.975 and 1.0. After multiplying with 0.877, these values are plotted with a dashed line in Fig. 15(b), which also includes the values of the nominal compressive strengths of *unreinforced* and *fully-reinforced* specimens computed using AISC360-10, as well as the test data in the same format used in Fig. 15(a). Using the proposed design equation defined in Eq. (4), the nominal compressive strengths of B60P3 specimens are also computed and added to the plot, in solid line, in Fig. 15(b). It is clear from Fig. 15(b) that all B60P3 specimens experienced inelastic buckling. The experimentally-determined values of strengths are much smaller than the nominal elastic buckling loads ($0.877P_e$); the difference increases as the reinforcement length ratio increases. The linear design equation proposed in Eq. (4) seems to predict, with sufficient accuracy, the compressive strength of all *partially-reinforced* B60 specimens, including the *nearly fully reinforced* specimens (B60P3L4 specimens).

Table 3 compares the strength predictions of the proposed linear equation ($P_{max,prop}$) with the experimental results ($P_{max,exp}$) for all test specimens. The ratios of the predicted values to the experimental values are also presented in the last column of the table, which shows, in general, a good agreement. The maximum difference between the predicted and experimental values is no more than 9%, if B40P3L4 specimens, two of which failed prematurely most probably due to the high localized bearing stresses at the unreinforced ends, are *not* included in the comparison.

Table 3 Comparison of strength predictions of the proposed design equation (Eq. (4)) with average experimental results

Test Specimen	$s=L^*/L$	$P_{max,exp}$ (kN)	$P_{max,prop}$ (kN)	$P_{max,prop}$ / $P_{max,exp}$
B40P0L0	0	104.39	106.60	1.02
B40P3L1	0.25	123.66	131.84	1.07
B40P3L2	0.5	146.10	157.09	1.08
B40P3L3	0.75	185.50	182.34	0.98
B40P3L4	0.98	157.64	205.06	1.30
B60P0L0	0	225.27	240.19	1.07
B60P3L1	0.25	281.42	274.32	0.97
B60P3L2	0.5	283.31	308.45	1.09
B60P3L3	0.75	351.20	342.59	0.98
B60P3L4	0.98	354.68	373.30	1.05

4. Conclusions

This paper presents an experimental study on the behavior of axially-loaded steel RHS compression members reinforced partially along their length with steel plates. Two sets of test specimens were prepared from two different RHS sections; 100×40×4 and 100×60×4mm, which lead, respectively, to the slenderness ratios of 125 and 83 for the reference (unreinforced) test specimens. The test specimens in each set were reinforced by welding 90×3mm steel plates over their larger faces in four different length ratios ($s=L^*/L$, where L^* and L are the length of the reinforcing plates and the column, respectively); 0.25, 0.50, 0.75, 0.975. The applied reinforcement increases the cross sectional area of the test specimens by about 50% in both sets. On the other hand, the increase in minor-axis moment of inertia, which governs the buckling behavior, is 94% for the 40-mm wide (B40) specimens and 78% for the 60-mm wide (B60) specimens. The basic material properties of the slender test specimens (i.e., the modulus of elasticity, offset yield strength and ultimate strength under compression) were determined using stub-column tests. Based on the limited experimental data and observations during the tests, the following conclusions may be drawn:

- The stub-column tests reveal that the basic mechanical properties of the composite (reinforced) sections are very close to those of the reference (unreinforced) sections for both tested tubes; the variation is not more than 6%. The effect of welding on mechanical properties appears to be very small in the reinforced specimens. The axial stress-strain curves for the reference stub-column specimens show gradual transition from linear elastic behavior to yield plateau, which verifies the existence of built-in residual stresses in the tested cold-formed tube sections. It is noteworthy that the stress-strain curves for most reinforced stub-column specimens begin to deviate from linearity at smaller stress levels, which can be attributed to the change of local buckling behavior on the reinforced webs of the tubes. It is believed that the buckling of each component (reinforcing plate and tube wall) did not occur, in general, simultaneously and in the same direction.
- The slender column tests show that the average percent

increase in axial capacity is 19, 40, 78, 51% for B40 specimens; 25, 26, 56, 58% for B60 specimens, for the reinforcement length ratios of *s*=0.25, 0.50, 0.75 and 0.975, respectively. Similarly, the average percent increases in elastic axial stiffness are 13, 30, 53 and 37% for B40 specimens and 19, 19, 22 and 32% for B60 specimens, for the same length ratios. For all specimens, the increase in stiffness is smaller than the increase in strength, which can be attributed to the fact that the increase in cross sectional area is smaller than the increase in moment of inertia in the tested reinforcement. The applied reinforcement is, in general, more effective on B40 specimens than B60 specimens since welding 3-mm thick steel plates to the larger sides of the tubes results in greater increase in moment of inertia, and consequently greater decrease in slenderness ratio, in B40 specimens.

• The slender column tests also show that similar to the unreinforced specimens, the partially-reinforced specimens failed due to excessive overall buckling; however, full-length buckling was typically followed by buckling observed at either the top or bottom unreinforced segment of the specimen. In this failure mode, the deformed shapes of the specimens were usually not symmetric about the mid-height. In some cases, local buckling and yielding were also observed at the section where the cross section changed abruptly. Contrary to the expectations, the strength and stiffness of nearly-fully reinforced B40 ($L^*=0.975L$) specimens are less than those of ¾-length reinforced B40 ($L^*=0.75L$) specimens. This is attributed mostly to the premature failure of some of the nearly-fully reinforced specimens due to the excessive yielding taking place on the short unreinforced ends (i.e., a kind of bearing failure). Thus, it is strongly suggested that the reinforcement be applied either full length or with sufficient clearance left at the ends to avoid such premature failure if greater strength/stiffness increase is required in design.

• A linear design expression is proposed in the paper for the prediction of compressive strength of partially-reinforced steel RHS members. The proposed design expression requires computing the nominal compressive strengths of the unreinforced (*s*=0) and fully-reinforced (s=1) specimens using the provisions given in AISC 360-10 (2010) for uniform members and making linear interpolation between them to account for the partial reinforcement of the specimen. The stub-column material properties can be used while computing the nominal strengths of uniform columns.

Additional tests are needed to evaluate the effects of (i) the amount (thickness and width) and strength of the reinforcing plates, (ii) the length of the reinforcement, including the full-length reinforcement, (iii) the type of the reference cross section, including the sections with slender elements and (iv) the slenderness ratio of the reference cross section, on compressive behavior of partially-reinforced compression members, thoroughly. Future studies are also required to determine the behavior of the partially-reinforced compression members under reversed cyclic loading if they are to be used in seismic-prone regions.

Acknowledgments

The research described in this paper was financially supported by the Kocaeli University Research Fund (Project No: 2012/92HDP and 2013/120HDP).

References

AISC360-10 (2010), *Specification for Structural Steel Buildings*, American Institute of Steel Construction; Chicago, Illinois.

Bhowmick, A.K. and Grondin, G.Y. (2016), “Limit state design of steel columns reinforced with welded steel plates”, *Eng. Struct.*, **114**, 48-60.

Brown, JH. (1988), “Reinforcing loaded steel compression members”, *Eng. J. AISC*, **Fourth Quarter,** 161-168.

Cuhadaroglu Pinarbasi, S., Akpinar, E., Okay, F., Meydanli Atalay, H. and Ozden, S. (2012), “Analytical, numerical and experimental studies on stability of three-segment compression members with pinned ends”, *Advances in Computational Stability Analysis*, Ed. Coskun S B, Intech, 91-114.

Fan, H.G., Chen Z.P., Feng W.Z., Zhou, F., Shen, X.L. and Cao, G.W. (2015), “Buckling of axial compressed cylindrical shells with stepwise variable thickness”, *Struct. Eng. Mech.*, **54**(1), 87-103.

Galambos, T.V. (1998), *Guide to Stability Design Criteria for Metal Structures*, 5th Edition, John Wiley and Sons, New York, USA.

Kus, J. (2015), “Lateral-torsional buckling steel beams with simultaneously tapered flanges and web”, *Steel Compos. Struct.*, **19**(4), 897-916.

Liu, S.W., Bai, R. and Chan, S.L. (2016), “Second-order analysis of non-prismatic steel members by tapered beam-column elements”, *Struct*., **6**, 108-118.

Marques, L., Da Silva, L.S. and Rebelo, C. (2014), “Rayleigh-Ritz procedure for determination of the critical load of tapered columns”, *Steel Compos. Struct.*, **16**(1), 45-58.

Nagaraja Rao, R.N. and Tall, L. (1962), “Columns reinforced under load”, Fritz Laboratory Report No. 286.1; Lehigh University Institute of Research, Lehigh University.

Park, J.S. (2004), “Lateral buckling formula of stepped beams with length-to-height ratio factor”, *Struct. Eng. Mech.*, **18**(6), 745-757.

Park, J.S. and Park, Y.S. (2013), “Inelastic lateral-torsional buckling strengths of stepped I-beams subjected to general loading condition”, *Struct. Eng. Mech.*, **48**(2), 275-289.

Pinarbasi, S., Okay, F., Akpınar, E. and Erdogan, H. (2013), “Stability analysis of two-segment stepped columns with different end conditions and internal axial loads”, *Math. Probl. Eng.*, **2013**, Article ID 858906.

Rajasekaran, S. and Wilson, A.J. (2013), “Buckling and vibration of rectangular plates of variable thickness with different end conditions by finite difference technique”, *Struct. Eng. Mech.*, **46**(2), 269-294.

Ren, Q.X., Han, L.H., Hou, C. and Hua, Y.X. (2017), “Experimental behavior of tapered CFST columns under combined compression and bending”, *J. Constr. Steel Res.*, **128**, 39-52.

Saka, M.P. (1997), “Optimum design of steel frames with tapered members”, *Comput. Struct*., **63**(4), 797-811.

Shaat, A. and Fam, A.Z. (2009), “Slender steel columns strengthened using high modulus CFRP plates for buckling

control", *J. Compos. Constr.*, ASCE, **13**(1), 2-12.
Singh, K.V. and Li, G. (2009), "Buckling of functionally graded and elastically restrained non-uniform columns", *Compos. Part B-Eng.*, **40**, 393-403.
Surla, A.S., Kang, S.Y. and Park, J.S. (2015), "Inelastic buckling assessment of monosymmetric I-beams having stepped and non-compact flange sections", *J. Constr. Steel Res*, **114**(325-337), 146-148.
Tall, L. (1989), "The reinforcement of steel columns", *Eng. J. AISC*, **First Quarter**, 33-37.
Tide, R.H.R. (1990), "Reinforcing steel members and the effects of welding", *Eng. J. AISC*, **Fourth Quarter**, 129-131.
Timoshenko, S.P. and Gere, J.M. (1961), *Theory of Elastic Stability*, 2nd edition, McGraw-Hill, New York, USA.
Wu, Z. and Grondin, G.Y. (2002), "Behaviour of steel columns reinforced with welded steel plates", Structural Engineering Report 250; Department of Civil and Enviromental Engineering, University of Alberta.
Zhang, X., Zhang, H. and Wen, Z. (2015), "Axial crushing of tapered circular tubes with graded thickness", *Int. J. Mech. Sci.*, **92**, 12-23.

CC